

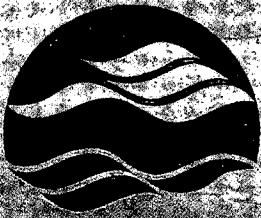
02-021



Environment  
Canada

Environnement  
Canada

Canada



NATIONAL WATER  
RESEARCH INSTITUTE

INSTITUT NATIONAL DE  
RECHERCHE SUR LES EAUX

TD  
226  
N87  
no.  
02-021

Over-lake meteorology and estimated  
bulk heat exchange of Great Slave Lake  
in 1998 and 1999

William M. Schertzer, Wayne R. Rouse,  
Peter D. Blanken and Anne E. Walker

NWRI Contribution # 02-021

## Over-Lake Meteorology and Estimated Bulk Heat Exchange of Great Slave Lake in 1998 and 1999

WILLIAM M. SCHERTZER

*Aquatic Ecosystem Impacts Research Branch, National Water Research Institute, Burlington, Ontario, Canada*

WAYNE R. ROUSE

*School of Geography and Geology, McMaster University Hamilton, Ontario, Canada*

PETER D. BLANKEN

*Department of Geography and Environmental Studies, University of Colorado, Boulder, Colorado*

ANNE E. WALKER

*Climate Research Branch, Meteorological Service of Canada, Downsview, Ontario, Canada*

(Manuscript received 26 September 2002, in final form 19 February 2003)

### ABSTRACT

Meteorological and thermistor moorings were deployed in Great Slave Lake during the Canadian Global Energy and Water Cycle Experiment (GEWEX) Enhanced Study (CAGES) in 1998 and 1999. Large-scale meteorology included influence from a record ENSO extending from 1997 to mid-1998. Meteorological variables varied across the lake especially during the lake-heating phase after ice breakup. Generally higher over-lake air temperature and surface water temperatures occurred in 1998, but larger vapor pressure gradients over water and ~8% higher solar radiation was observed in 1999. Although wind speed averages were similar in both years, nearly 30% more over-lake storms with winds  $>10 \text{ m s}^{-1}$  occurred in 1998. High sensitivity of the lake temperatures to surface wind forcing was observed in 1998 in the spring warming phase. Passive microwave imagery [from the Special Sensor Microwave Imager (SSM/I)] at 85 GHz showed a record 213 ice-free days in 1998 compared to 186 days in 1999. The extended ice-free period in 1998 significantly influenced lake temperature and heat content. Maximum heat content occurred on 5 August in 1998 ( $2.61 \times 10^{19} \text{ J}$ ) compared to 23 August in 1999 ( $2.22 \times 10^{19} \text{ J}$ ). The daily heat content formed the basis for deriving a bulk heat exchange. Five-day-averaged bulk heat exchange generally fluctuated between means of 282 (spring) to -225 (fall)  $\text{W m}^{-2}$  in 1998, compared to a smaller range of 171 (spring) to -202 (fall)  $\text{W m}^{-2}$  in 1999. Good correspondence between the bulk heat exchange based on lakewide heat content and computed heat flux at Inner Whaleback Island gives confidence in the seasonal heat flux and the heat content methodology. The seasonal trend and magnitudes of heat contents and bulk exchanges derived in this analysis form the basis for future research on the interannual variability in lakewide heat budgets and for developments leading to coupled climate-lake models.

### 1. Introduction

The Mackenzie River basin has experienced some of the largest temperature increases compared to other locations in the world (Stewart et al. 1998). This has necessitated research to understand the magnitude of and processes controlling heat and mass exchange from the various surfaces in the basin (Rouse et al. 2002). It is a necessary step in the development of models that can be applied to predict climate impacts. This research fo-

cuses on Great Slave Lake as part of the Mackenzie Global Energy and Water Cycle Experiment (GEWEX) Study (MAGS). Understanding the role of lakes within this northern climate system is one of the goals of the Canadian GEWEX Enhanced Study (CAGES).

An analysis of Advanced Very High Resolution Radiometer (AVHRR) data (Bussi eres 2001) shows that lakes of various sizes are particularly predominant in the eastern half of the Mackenzie basin (Fig. 1a). Other than research investigations on a small sample of these lakes, little is known of the seasonal distributions, magnitudes, and interannual variability of the over-lake hydrometeorology, thermal responses, heat content, or heat exchanges associated with these water bodies.

Characteristics of the climate variability and temper-

*Corresponding author address:* William M. Schertzer, Aquatic Ecosystems Impacts Research Branch, National Water Research Institute, 867 Lakeshore Rd., Burlington, ON L7R 4A6, Canada.  
E-mail: william.schertzer@ec.gc.ca

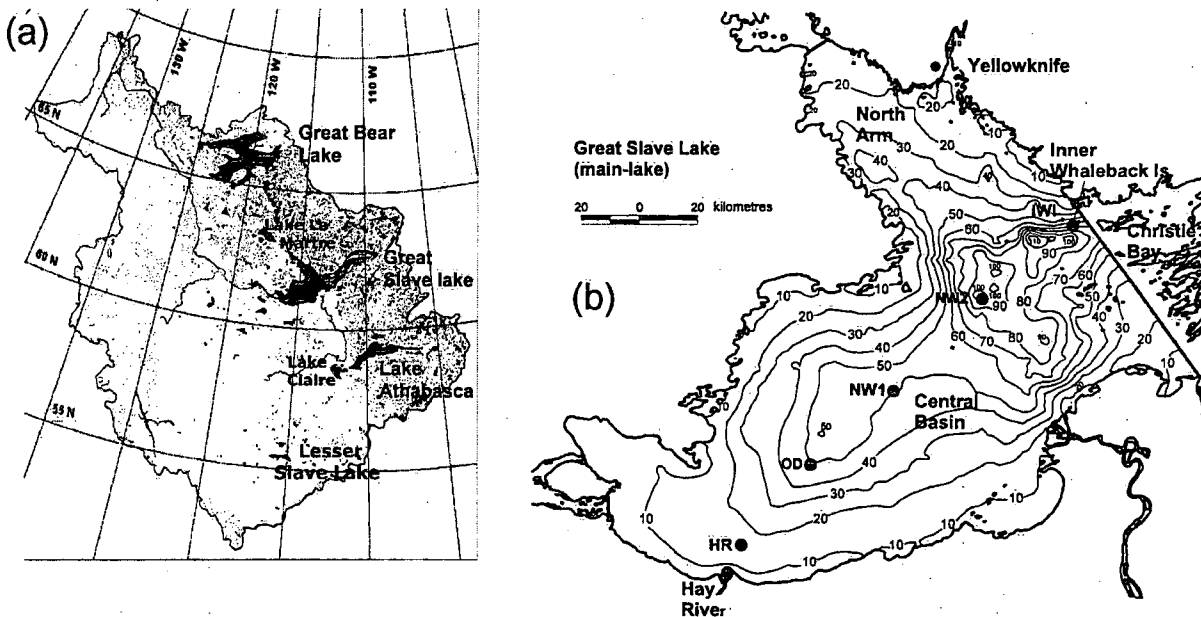


FIG. 1. (a) The distribution of lakes within the Mackenzie basin based on AVHRR 1-km resolution (based on Bussi eres 2001). (b) Bathymetry of the main lake section of Great Slave Lake, and location of meteorological and temperature moorings in 1998 and 1999 (based on Schertzer 2000).

ature of Great Slave Lake were initially described by Rawson (1950), based on a series of ship surveys in 1947 and 1948. Recently, as part of MAGS, detailed observations of hydrometeorological and limnological components have been conducted (Blanken et al. 2000; Rouse et al. 2000a,b; Schertzer et al. 2000a), which has extended the initial research of Rawson (1950). The main objectives of this paper are (a) to describe and compare the over-lake meteorological conditions in 1998 and 1999, (b) to quantitatively describe the seasonal temperature cycle, thermal structure, and heat content of Great Slave Lake in the CAGES period, and (c) to estimate the bulk heat exchange of the lake based on the heat content. This paper provides the first approximation of the total annual bulk heat exchange derived from the heat content approach and is compared with a computed heat exchange calculated from the energy budget (Rouse et al. 2003).

## 2. Site, measurements, and techniques

### a. Lake bathymetry

Great Slave Lake is one of three large lake systems within the Mackenzie basin. It is located between Great Bear Lake and Lake Athabasca (Fig. 1a). The surface area of Great Slave Lake is 27 200 km<sup>2</sup> with a total volume of 1070 km<sup>3</sup> (van der Leeden et al. 1990). The lake consists of a central basin, a northern arm, and an eastern arm called Christie Bay. In this analysis we concentrate on the main lake, defined here as consisting of the central basin plus the northern arm (Fig. 1b).

A detailed description of the derivation of the bathymetry for Great Slave Lake (main lake) is provided in Schertzer (2000) using 2227 depth soundings. Based on a 2 km × 2 km grid bathymetry, the main lake has a surface area of 18 500 km<sup>2</sup> and an integrated volume of 596 km<sup>3</sup>. The maximum depth of the main lake is 187.7 m and the mean depth is 32.2 m.

### b. Meteorological and temperature moorings

Over-lake meteorological observations on Great Slave Lake were conducted during CAGES from Inner Whaleback Island (Rouse et al. 2000a) and from meteorological buoys (Schertzer et al. 2000a) forming a cross-lake transect extending from Hay River to Inner Whaleback Island (Fig. 1b). Meteorological observations included air temperature, water surface temperature, relative humidity, wind speed, wind direction, and solar radiation. Observations were recorded at 10-min intervals at sites HR, NW1, NW2, IWI, and hourly at OD. All data were processed to hourly and daily averages and wind directions were corrected to magnetic north.

Water temperature moorings were also deployed at each of the sites (Fig. 1b). In 1998, a combination of temperature loggers (StowAway Optic, StowAway TidbiT, and Brancker loggers) were used (Table 1a). In 1999, moorings were equipped with StowAway TidbiT sensors exclusively. Sensor depths were standardized to allow for comparability of thermal profiles (Table 1b), and observations were recorded at 15-min intervals.

TABLE 1. Details of temperature moorings installed in Great Slave Lake during CAGES 1998–99 summer and winter field programs.

(a) Temperature loggers and characteristics													
Logger type	Accuracy (°C)		Max depth (m)		Temperature range (°C)								
StowAway Optical	±0.2		30.5		–5 to +37								
Stowaway TidbiT	±0.2		304.8		–5 to +37								
Brancker TR-1000	±0.05		1000		–5 to +35								
Brancker XL-100	±0.15		1000		–20 to +50								

(B) Thermistor mooring measurement depths														
	Depth (m)													
	0	2	5	7.5	10	13.5	15	20	25	30	40	50	75	100
HR	*		*	*	*		*							
OD	*	*	*	*	*	*	*	*	*	*	*	* 56 m		
NW1	*	*	*	*	*	*	*	*	*	*	*	*	* 60 m	
NW2	*	*	*	*	*	*	*	*	*	*	*	*	*	* 121 m
IWI	*		*		*		*		*		*	* 50 m		

(c) Winter thermistor mooring measurement depths										
	Depth (m)									
	12	14	16	20	25	30	40	50	75	100
OD	*	*	*	*	*	*	*	* 54.5 m		
NW2	*	*	*	*	*	*	*	*	*	* 100 m

A bulk surface temperature was observed from each of the meteorological buoys. At NW1 and NW2 a thermistor was mounted at the side of a 3-m geodyne toroidal buoy within a thermal shield at a depth of 25 cm below the water surface. We use a Campbell Scientific model 107B thermistor with accuracy of  $\pm 0.1^\circ\text{C}$  over the range  $-24^\circ\text{C}$  to  $+48^\circ\text{C}$ . The thermistor time constant is  $200\text{ s} \pm 10\text{ s}$ , which significantly dampens the effect of buoy motions on the temperature observation. At OD, the water temperature sensor is mounted on the inside bottom of a 3-m discus buoy hull located 78.4 cm below the water line (AXYS 1996). Temperature accuracy is  $0.15^\circ\text{C}$  over the range  $-35^\circ$  to  $+35^\circ\text{C}$ . The surface water temperature does not represent "skin" temperature, which is often derived from infrared thermometer. Rather, the observations represent a bulk surface temperature measurement common in physical limnology and oceanography.

Winter temperature moorings were installed at OD in 1998–99 and at OD and NW2 in 1999–00. Ice has been observed to crack and tilt downward (raft) up to 25 m in other large lakes, such as Lake Erie. Rafting of ice can either pull a mooring off site or effectively destroy it. Because little is known of the ice dynamics in Great Slave Lake, thermistors were deployed from a depth of 12 m from the surface to 1 m from the lake bottom to minimize the potential danger of ice rafting (Table 1c). We have assumed isothermal conditions above the 12-m depth for the winter experiment in order to facilitate computation of the winter heat content over the whole lake volume.

#### c. Passive microwave (SSM/I) techniques for lake ice determinations

Passive microwave imagery (SSM/I) at the 85-GHz range (Walker and Davey 1993) can discriminate be-

tween ice cover and open water. The SSM/I technique is applicable at any time of the day, in all weather conditions, and provides a resolution of 12.5 km from the 85-GHz channel. SSM/I brightness patterns have been processed over the CAGES period to provide dates for ice break up and freeze up in Great Slave Lake (Walker et al. 1999).

#### d. Wind, vapor pressure, and atmospheric stability computation

Wind speeds across the lake transect were measured at different heights (HR: 3.0 m; OD: 4.27 m; NW1: 4.0 m; NW2: 4.0 m; and IWI: 8.52 m) and were converted to a common height of 8 m, based on the U.S. Army Corps of Engineers (1984) formulation

$$U_8 = U_m(z_8/z_m)^{1/7}, \quad (1)$$

where  $U_8$  = wind speed ( $\text{m s}^{-1}$ ) at a height of 8 m ( $z_8$ ) and  $U_m$  = measured wind speed ( $\text{m s}^{-1}$ ) at the observed height ( $z_m$ ). Averaged atmospheric conditions were near neutral during most of the summer (see section 3a) and no corrections for stability were incorporated.

Wind stress vectors were superimposed on the temperature isotherm sequences to provide an indication of the response to atmospheric forcing. The wind stress was computed as

$$\tau = \rho_a C_D U_8^2, \quad (2)$$

where  $\tau$  is the wind stress ( $\text{N m}^{-2}$ ),  $\rho_a$  is air density,  $C_D$  is the drag coefficient ( $1.3 \times 10^{-3}$ ), and  $U_8$  is the wind speed at 8 m ( $\text{m s}^{-1}$ ).

Richardson number has been computed based on Oke (1987). Vapor pressures were computed based on Pruppacher and Klett (1980).

TABLE 2. Statistical summary of measured over-lake meteorological components during CAGES. Averages are computed for the Great Slave Lake stations over the Jun–Oct period for 1998 and 1999. For comparison, Jun–Oct averages are provided for Yellowknife Airport based on climate normals 1942–90.

Variable	Unit	Year	Mean	Max	Min	Std dev	YZF
Atmospheric pressure	hPa	1998	991.9	1013.8	958.3	8.2	986.5
		1999	992.5	1011.7	968.7	8.2	
		$\Delta$	-0.06	2.1	-10.4	0.0	
Air temperature	$^{\circ}\text{C}$	1998	12.9	23.5	0.3	4.8	9.8
		1999	9.7	18.4	-2.7	4.8	
		$\Delta$	3.2	5.1	3.0	0.0	
Surface temperature	$^{\circ}\text{C}$	1998	12.9	20.5	3.5	4.1	—
		1999	9.3	16.9	0.2	3.8	
		$\Delta$	3.6	3.6	3.3	0.3	
Wind speed	$\text{m s}^{-1}$	1998	6.8	15.6	1.5	2.9	4.3
		1999	6.7	13.7	2.7	2.6	
		$\Delta$	0.1	1.9	-1.2	0.3	
Relative humidity	%	1998	79.2	94.3	61.4	6.7	77.6
		1999	77.7	91.9	57.8	6.8	
		$\Delta$	1.5	2.4	3.6	-0.1	
Solar radiation	$\text{W m}^{-2}$	1998	161.5	328.2	12.3	89.8	—
		1999	176.0	345.7	4.2	99.6	
		$\Delta$	-14.5	-17.5	8.1	-9.8	

$\Delta$ , represents value 1998 minus 1999.

YZF; represents Yellowknife Airport. Jun–Oct climate normal 1942–90.

#### e. Heat content and bulk heat exchange

A time series of daily heat content in the main lake is derived for 1998 and 1999. We apply daily-averaged temperature vs depth observations from each temperature mooring to a  $2 \text{ km} \times 2 \text{ km}$  grid bathymetry with inverse distance squared weighting for each 1-m depth interval from the surface to the lake bottom (Schertzer 2000). The computed heat in each grid element is

summed to derive the heat content for each day. We compute the daily change in the lake heat content to represent a bulk exchange at the lake surface.

### 3. General characteristics of the over-lake meteorology during CAGES

#### a. Over-lake meteorology from June to October in 1998 and 1999

Over-lake daily-averaged meteorological conditions for 1998 and 1999 are computed for the period June–October generally corresponding to the ice-free period. Basic statistics for measured variables are shown in Table 2, including averaged 1942–90 climate normals from Yellowknife Airport, Yellowknife, Northwest Territories, Canada. Mean daily variability is shown in Figs. 2–5.

Multivariate El Niño–Southern Oscillation (ENSO) index indicates the occurrence of a record ENSO from 1997 to mid-1998. The CAGES period from June 1998 to September 1999 was largely characterized by a transition to La Niña conditions, and included warmer than average surface air temperatures and considerable variability in weather across the Mackenzie basin (J. R. Gyakum 2002, personal communication).

Atmospheric pressure means were similar between 1998 and 1999 (Fig. 2a). Over-lake air temperature for 1998 was significantly higher than for 1999 up to mid-August, with largest differences ( $\sim 10^{\circ}\text{C}$ ) observed at the beginning of July (Fig. 2b). Mean air temperature in 1998 was nearly  $3^{\circ}\text{C}$  higher than at Yellowknife Airport, while 1999 values were nearly equal (Table 2). Average surface water temperature for 1998 was  $3.5^{\circ}\text{C}$  higher than in 1999 (Fig. 2c). Substantial differences

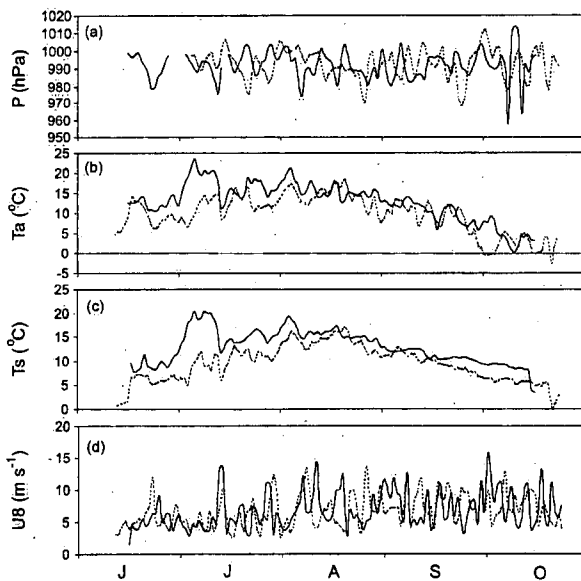


FIG. 2. Comparison between daily lakewide-averaged (a) atmospheric pressure, (b) air temperature, (c) surface water temperature, and (d) wind speed. Observations in 1998 (solid line) and 1999 (dashed line) are indicated.

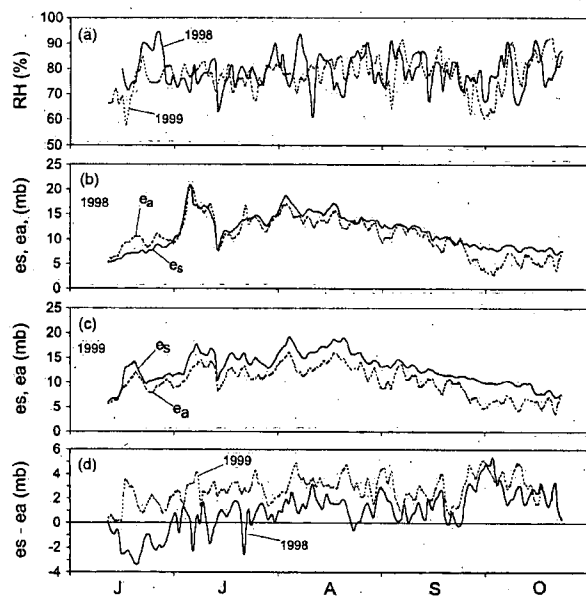


FIG. 3. Comparison between (a) relative humidity, (b) daily lakewide-averaged saturation and ambient vapor pressures for 1998, and (c) daily lakewide-averaged saturation and ambient vapor pressures for 1999, and (d) vapor pressure difference ( $e_s - e_a$ ) for 1998 and 1999.

are seen in the warming phase from mid-June to August, with large differences up to  $10^{\circ}\text{C}$  for a 2-week period in the beginning of July. Similar over-lake wind speed averages for 1998 and 1999 (Fig. 2d) are  $2.5 \text{ m s}^{-1}$  higher than the long-term mean at Yellowknife Airport. Approximately 18 episodes had daily average winds  $>10 \text{ m s}^{-1}$  in 1998 compared to 14 in 1999. Large differences in relative humidity were observed during late June (Fig. 3a) where 1998 values reached 20% higher than in 1999. Saturation minus ambient vapor pressure,  $e_s - e_a$ , was consistently larger in 1999 compared to 1998 (Fig. 3d). In the latter half of June 1998, the vapor pressure difference is negative, which is indicative of lake heat gains through condensation.

Variation of air and water temperature difference,  $T_a$ ,

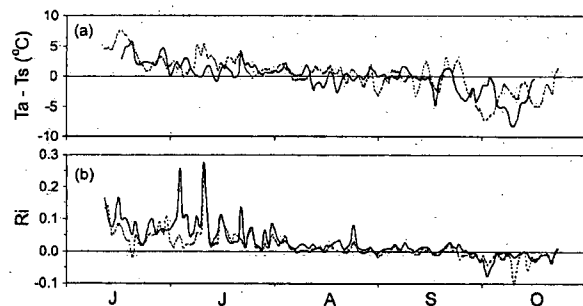


FIG. 4. Comparison between daily lakewide-averaged (a) air minus water temperature and (b) atmospheric stability based on the Richardson number. Observations in 1998 (solid line) and 1999 (dashed line) are indicated.

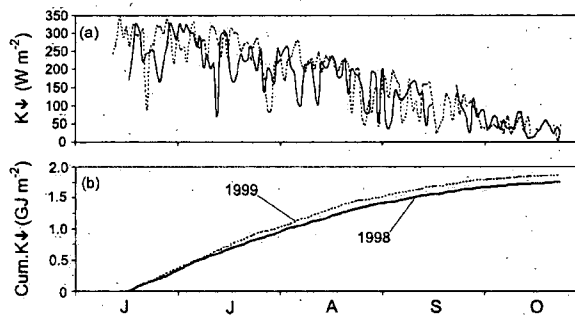


FIG. 5. Comparison between daily lakewide-averaged (a) solar radiation and (b) cumulative solar radiation income for concurrent periods. Observations in 1998 (solid line) and 1999 (dashed line) are indicated.

and the Richardson number ( $R_i$ ) show generally stable atmospheric conditions from June to July (Figs. 4a and 4b) and unstable conditions in the cooling phase as air temperatures are lower than water surface temperature. The mean daily value of  $R_i$  was slightly larger in 1998 ( $R_i = 0.03$ ) compared to 1999 ( $R_i = 0.02$ ).

Mean daily income of solar radiation (Fig. 5a) was lower in 1998 compared to 1999. Cumulative totals of incoming solar radiation for concurrent periods from mid-June to mid-October (Fig. 5b) show that approximately 8% more solar radiation was received in 1999 ( $1.22 \times 10^9 \text{ J m}^{-2}$ ) compared to 1998 ( $1.13 \times 10^9 \text{ J m}^{-2}$ ).

#### b. An example of the spatial variability of over-lake meteorology: 1998

Spatial variability of over-lake meteorology is shown in Fig. 6. For June–August, air temperature and water temperature at the nearshore station HR was higher than midlake. In spring, after ice break up, the differences between shallow nearshore and deeper offshore stations is particularly apparent. Whereas the surface water temperature nearshore approaches  $10^{\circ}\text{--}15^{\circ}\text{C}$ , the deepest sites at NW1 and NW2 may still be below the temperature of maximum density ( $4^{\circ}\text{C}$ ). The month of June is seen as a period of rapidly increasing water temperatures. Spatial differences in wind speed were also evident. As expected, wind speeds tend to be higher mid-lake compared to nearshore due to fetch considerations. Particularly evident is the number of high-wind episodes at all stations (Schertzer et al. 2000a).

## 4. Response of lake temperature and thermal structure in CAGES

### a. Seasonal temperature cycle

A complete annual temperature cycle has been recorded for the first time for this lake extending from mid-June 1998 to December 1999 (Fig. 7). Great Slave Lake is a dimictic lake, which means that it passes

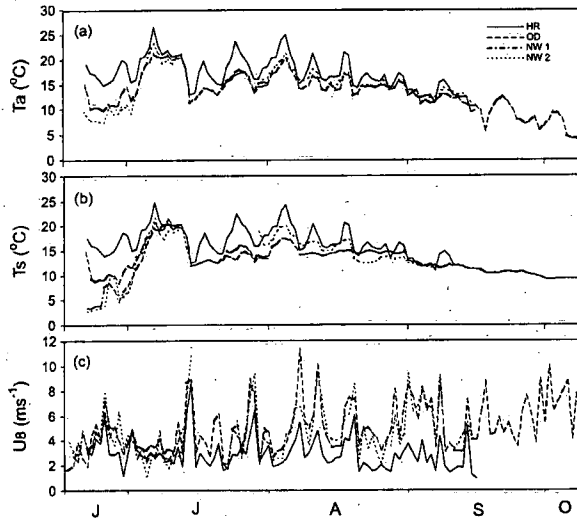


FIG. 6. An example of the spatial variability in (a) air temperature, (b) surface water temperature, and (c) wind speed for over-lake buoys along the cross-lake transect in Great Slave Lake during the ice-free period of 1998.

through the temperature of maximum density for water (4°C) twice a year with complete overturn occurring once in the spring and again in the fall. Based on 1998 and 1999 surface water temperatures (Fig. 7), the spring overturns occur in June and the fall overturn occurs in October.

Yellowknife 30-yr climatology for October–April shows mean monthly air temperatures ranging from -1° to -25°C with minimum values from -27° to -47°C.

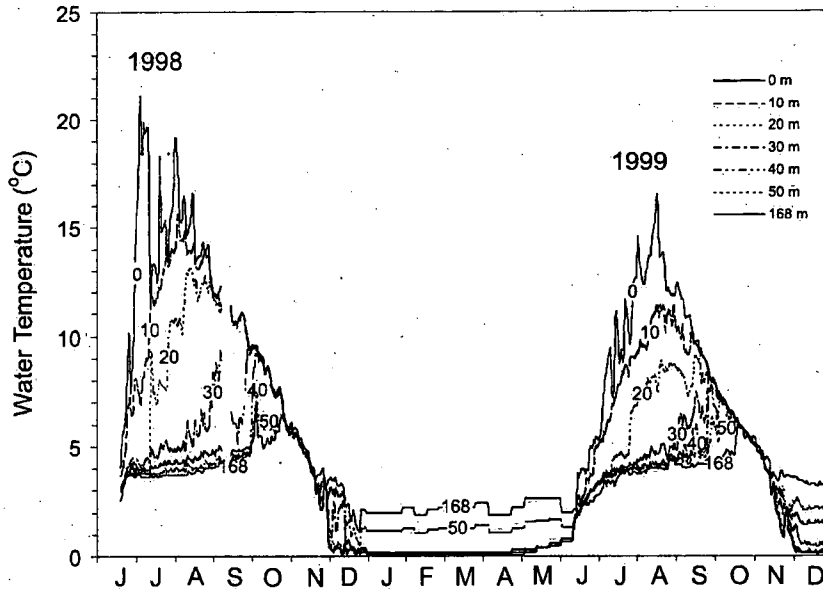


FIG. 7. Seasonal water temperature distribution in Great Slave Lake from Jun 1998 to Dec 1999. Station data have been extended over the 2 km × 2 km grid bathymetry to a maximum depth of 168 m.

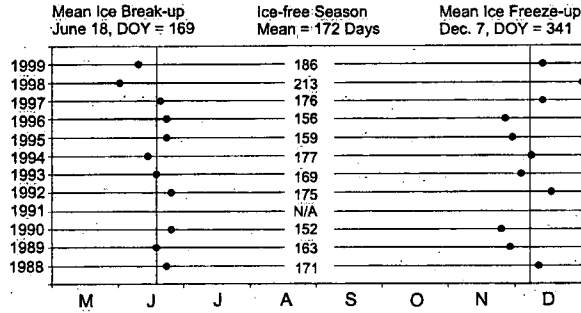


FIG. 8. Dates of ice breakup and freezeup, and corresponding ice-free days for the long-term period 1988–99 (based on Walker et al. 1999). Note that the ice-free periods for the CAGES years 1998 and 1999 are the longest for the 12-yr series.

These temperatures result in complete lake ice cover. Lake temperatures during winter can reach minimums (~0.1° to 1.0°C). Temperatures at 1 m above the lake bottom were observed at 1.5°–2.5°C, suggesting a possible release of heat from the lake sediments.

Ice cover effectively decouples the lake–atmospheric exchange, and the length of the ice-free season indicates climatic conditions. Based on 1988–99, the main lake is expected to be ice free by 18 June and ice freeze over is expected on 7 December, with an average ice-free period of 172 days (Fig. 8) (Walker et al. 1999). Over the period 1988–99, the longest ice-free period (213 days) occurred in 1998. In 1998, spring air temperatures were observed to be as much as 3°C higher than normal. Walker et al. (1999) show that in 1998, extensive open-water areas are evident by 27 May, which is about 3

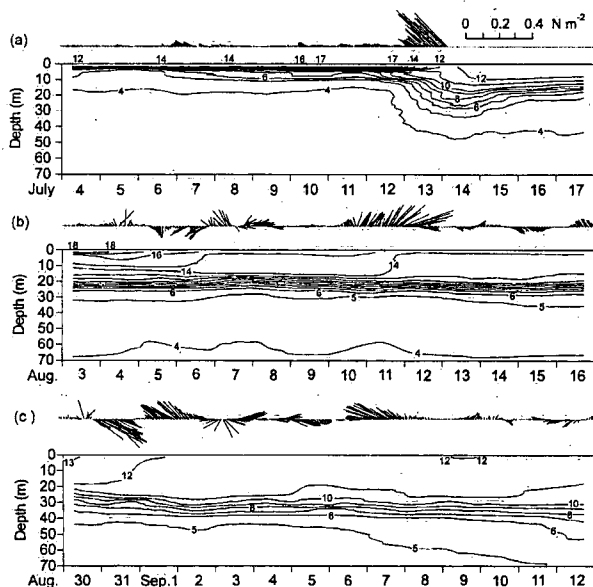


FIG. 9. An example of the thermal response of Great Slave Lake to surface wind forcing during (a) the beginning of thermal stratification 4–17 Jul 1998, (b) at the time of maximum temperature and heat content 3–16 Aug 1998, and (c) in the cooling phase 30 Aug–12 Sep 1998. Wind stress vectors are plotted relative to north.

weeks earlier than the average. In contrast, 1999 ice breakup in the main lake occurred on 10 June, nearly 15 days later than in 1998. The date of ice freeze up in 1998 was 31 December, resulting in 213 ice-free days. In comparison, the date of ice freeze up in 1999 was 14 December, resulting in 186 ice-free days.

Surface temperature (Fig. 6) shows time lags in spring warming in the deeper midlake compared to rapid warming in the shallower near shore after ice melt. Heat advected to the lake from major inflows, such as the Slave River, can be expected to have a local effect on water temperature, but the magnitude and spatial extent have not been evaluated. During spring under calm weather, a shallow ( $\sim 1$ – $2$  m), warm upper layer can develop in the midlake where the surface layer may be greater than  $10^{\circ}\text{C}$  warmer than in lower layers. The spatial variation in water temperature can affect surface heat fluxes. During spring, the total heat flux is dominated by high net radiation, contributing to lake heating (Schertzer et al. 2000b; Rouse et al. 2003). Spring vapor pressure differences (Fig. 3) and air–water temperature differences (e.g., Fig. 4) suggest that turbulent heat fluxes also vary across the lake.

Figure 7 shows large differences in the temperature structure of the lake during the thermally stratified season in 1998 compared to 1999. Warmer spring conditions in 1998 resulted in earlier ice melt, and also influenced rapid heating of the nearshore and near-surface layers midlake (Fig. 9). Maximum temperature in Great Slave Lake occurred in July ( $20.5^{\circ}\text{C}$ ) compared to mid-August at  $16.9^{\circ}\text{C}$  in 1999. Strong winds disrupted the

developing stratification in the 1998 spring heating phase (see section 4b). Rapid warming of the lake from ice melt to early July that occurred in 1998 resulted in higher temperatures later in the year, especially evident in the upper 50 m, compared to 1999.

Breakdown of thermal stratification can vary across a lake as a consequence of spatial differences in heat exchanges and winds. The lake became isothermal in 1998 and 1999 in October at approximately  $6^{\circ}\text{C}$  and progressive heat losses reached the temperature of maximum density ( $4^{\circ}\text{C}$ ) in mid-November (Fig. 7). After overturn, the lake enters a near 4-month period of minimum under ice temperatures. Observed winter temperatures ranging from  $\sim 0.1^{\circ}$  to  $0.5^{\circ}\text{C}$  in February is similar to that observed in Lake Erie (e.g. Schertzer et al. 1987) under complete ice cover.

*b. An example of lake thermal response to wind forcing in 1998*

Wind is a major factor influencing many thermal and hydrodynamic processes in large deep lakes (e.g. Boyce et al. 1989). We provide examples of the lake thermal response to wind forcing during three periods: lake heating, time of maximum heat storage, and during the cooling phase of 1998.

The effect of large storms on the temperature distribution in this lake is shown in Fig. 9a at the deep lake station NW2 from 4–17 July 1998. The main lake was essentially ice free on 25 May. Preceding temperature sequences indicate that the  $4^{\circ}\text{C}$  temperature isotherm has passed the deep station on 26 June 1998, and consequently, thermal stratification has begun at this location. The near-surface temperature increased from  $4^{\circ}\text{C}$  on 26 June to  $12^{\circ}\text{C}$  at the beginning of this sequence to maxima of  $\sim 17^{\circ}$  to  $20^{\circ}\text{C}$  by 12 July. The upper thermal layer was less than 5 m deep from the surface from 4–12 July. On 13 July, an intense storm with winds from the southeast resulted in wind stresses of the order  $0.3\text{ N m}^{-2}$ , which generated waves approaching 4 m (Schertzer et al. 2000a). The  $4^{\circ}\text{C}$  isotherm deepened from  $\sim 18$  to 45 m depth, and the surface temperature decreased from  $17^{\circ}$  to  $12^{\circ}\text{C}$ . Calmer winds after this period, indicated by adjacent buoys, were responsible for a partial recovery of the thermocline layer to a depth of 10–25 m. This event markedly affected the thermal stratification at this station for the 1998 heating season as the thermocline remained at the 15–25-m-depth to the period of maximum heat storage in mid-August.

The hourly temperature structure at NW2 is shown for the upper 70 m for the sequence 3–16 August 1998, which straddles the period of maximum heat content. Several high-wind events occurred throughout the period; however, unlike the early heating phase, high winds mainly affected the temperature of the upper layer. During 3–5 August, temperatures above the thermocline ranged from  $14^{\circ}$  to  $18^{\circ}\text{C}$  (surface to 15 m), and temperature in the thermocline region ranged between



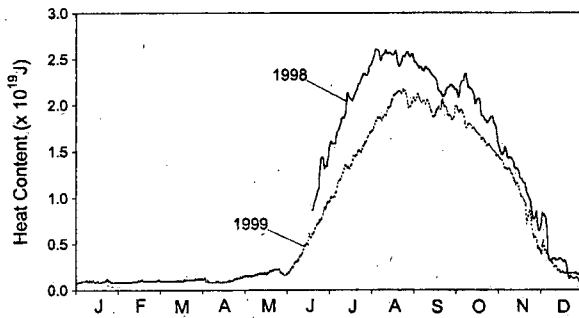


FIG. 10. Comparison of daily lakewide heat content for Great Slave Lake (mainlake) in 1998 and 1999.

6° and 13°C. High winds beginning on 5 August resulted in mixing temperatures in the upper layer to 14°C. High winds from 11–12 August continued to reduce the temperature of the upper mixed layer to 13°C. The thermocline generally ranged between 15- and 25-m depth.

After maximum heat storage, the lake begins to lose heat, largely as a result of radiative and turbulent heat losses and wind mixing (see Rouse et al. 2003). The sequence from 30 August to 12 September 1998 (Fig. 9c) occurs during the midstages of the cooling cycle. The combined effects of radiative and turbulent heat losses (see, Rouse et al. 2003) and high winds effectively result in increased heat losses to the atmosphere and deepening of the upper thermal layer. The upper mixed layer extends to below the 30-m depth at this location during this period. The lake continues to lose heat and becomes isothermal near the end of October in 1998 (Fig. 7).

## 5. Lakewide heat content and bulk heat exchange

### a. Lakewide heat content during CAGES

A complete heat content cycle was derived for 1999 and only for the period from mid-June onward for 1998 (Fig. 10). The most obvious difference between years is the larger heat content in the lake in 1998 compared to 1999. Maximum heat content was  $2.61 \times 10^{19}$  J on 5 August 1998 compared to  $2.22 \times 10^{19}$  J on 23 August 1999. The spring heat income is defined as the amount of heat gained by the lake from its minimum temperature to the temperature of maximum density (4°C). Because temperature observations in 1998 only began in June, we assume here that the minimum heat content in 1998 occurred at the same time as in 1999 on 4 January at  $6.56 \times 10^{17}$  J. Consequently, the spring heat income for 1998 was  $0.12 \times 10^{19}$  J compared to  $0.48 \times 10^{19}$  J in 1999. The summer heat income represents heating from the time of temperature of maximum density to the date of maximum heat content. The summer heat gain for 1998 ( $2.42 \times 10^{19}$  J) was significantly larger compared to ( $1.68 \times 10^{19}$  J) in 1999. The heat content range was  $2.54 \times 10^{19}$  J in 1998 compared to  $2.16 \times 10^{19}$  J in 1999. Heat contents show a pronounced asymmetry be-

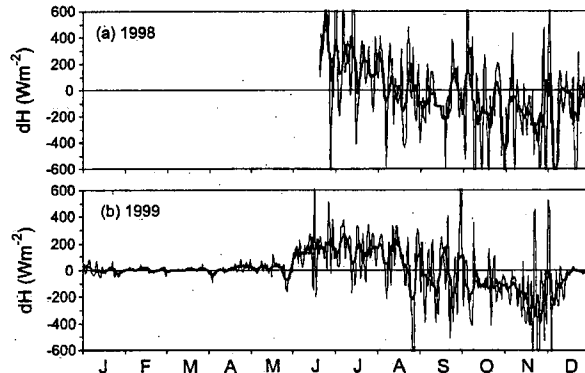


FIG. 11. An estimate of the total daily bulk heat exchange for Great Slave Lake (mainlake) for (a) 1998 and (b) 1999. Daily bulk heat exchange (light line) and 5-day mean exchange (superimposed, thick solid line) are plotted.

tween the heating and cooling rates, especially for 1998. Considering the period between the occurrence of the temperature of maximum density (4°C) to time of maximum heat storage, the rate of heat gain for 1998 was  $3.78 \times 10^{17}$  J day<sup>-1</sup>, considerably greater compared to  $2.36 \times 10^{17}$  J day<sup>-1</sup> for 1999. Considering the period from time of maximum heat content and the date of occurrence of the temperature of maximum density (4°C) in the fall, the rates of heat loss during the cooling phase were  $0.84 \times 10^{17}$  J d<sup>-1</sup> in 1998 and  $0.97 \times 10^{17}$  J in 1999.

### b. Bulk heat exchange based on computed heat content

We define a bulk heat exchange  $dH$  that represents the total heat gain or loss from the lake on a daily basis based on the heat content determinations shown in Figs. 11a and 11b. The bulk determination in this analysis assumes that all possible heat gains and losses are accounted for in the thermal observations that were used to derive the daily heat content (Fig. 10). Figures 11a and 11b show  $dH$  for 1998 and 1999, respectively. The fluxes on a daily basis show larger fluctuations compared to the 5-day running mean.

Several important characteristics of the heat exchange are apparent. During the ice-covered period (January–June), the exchange with the atmosphere was effectively nil, and changes in lake heat contents were very small and probably only influenced by such processes as hydrological discharges and release of heat from the sediments, including penetration of light through the ice cover (Walker and Davey 1993). Ice breakup from the end of May to early June resulted in rapid heat gain to the lake, which continued through June and into mid-August. The bulk heat exchange alternated between periods of heat gain and loss through mid-August to mid-September in response to high winds and progressive deepening of the upper mixed layer. Large negative bulk

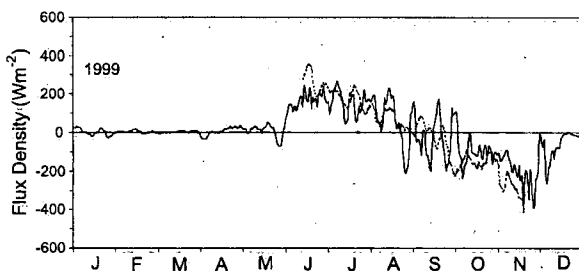


FIG. 12. Comparison of 5-day mean bulk heat exchange from heat content (solid line) with heat flux estimate computed at Inner Whaleback Island (dashed line) in 1999; 5-day means computed for IWI is based on heat fluxes provided by Rouse et al. (2003).

heat exchanges were more prevalent from mid-September onward to the beginning of December. Large heat losses in this period are related to deep mixing from high winds and higher turbulent heat losses (see Rouse et al. 2003).

Based on an arbitrary 25-day period in spring (26 June–July 21) and in the fall (21 November–16 December), the 5-day-averaged bulk heat exchange in 1998 generally fluctuated between 282 (spring) and  $-225$  (fall)  $\text{W m}^{-2}$  compared to a smaller range 171 (spring) and  $-202$  (fall)  $\text{W m}^{-2}$  of 1999. The large early spring heat fluxes for 1998 compared to 1999 show the effect of the warmer weather conditions associated with the intense El Niño.

### c. Comparison of bulk heat exchange with computed heat flux

Figure 12 shows a comparison between the 5-day mean bulk heat exchange determined from heat content computations in this paper, with a total heat flux computed from Inner Whaleback Island in 1999 based on detailed observations of radiative and turbulent exchanges from eddy correlation (Rouse et al. 2003; Blanken et al. 2000; Blanken et al. 2003). Rouse et al. (2003) defines a modified heat exchange expressed as the following:

$$Q_{ST} = Q^* - Q_E - Q_H \quad (3)$$

where  $Q_{ST}$  is the total heat exchange,  $Q^*$  is the net radiative exchange,  $Q_E$  is the latent heat flux, and  $Q_H$  is the sensible heat flux. The net radiation is defined as

$$Q^* = K\downarrow - K\uparrow + L\downarrow - L\uparrow, \quad (4)$$

where  $K\downarrow$  is the incoming global solar radiation,  $K\uparrow$  is reflected solar radiation,  $L\downarrow$  is incoming longwave radiation, and  $L\uparrow$  is the emitted longwave radiation. Equation (3) does not include minor energy sources, such as flux at the lake bottom or an advective component  $Q_V$ , to describe heat gains and losses resulting from hydrological exchanges (e.g., precipitation, inflows, outflows, and ice formation and decay). Research on large lakes, such as Lake Ontario (Pinsak and Rodgers 1981) and

Lake Erie (e.g. Derecki 1975), shows that  $Q_V$  is generally less than 2% of the total heat flux during the ice-free season (Schertzer 1997).

Both methodologies show similar magnitudes of lake heat gains during the spring and heat losses during the fall (Fig. 12). As suggested in Fig. 6, there can be spatial variability in hydrometeorological variables across the lake. As such, the day-to-day differences between the bulk heat exchange and the computed surface flux at Inner Whaleback Island are probably due to locational factors. The good agreement in the seasonal characteristics (shown in Fig. 12) gives confidence in our methods for calculating the lake heat storage, and also offers a verification on the computed heat fluxes from Inner Whaleback Island.

## 6. Discussion and conclusions

This research provides a description of the over-lake meteorology, the seasonal temperature cycle, thermal structure, heat content, and bulk heat exchange of Great Slave Lake in response to climate conditions in the CAGES period of 1998 and 1999.

Weather during the early part of 1998, was influenced by a record El Niño that extended from 1997 to mid-1998 with La Niña conditions prevalent for the remainder of CAGES (J. R. Gyakum 2002, personal communication). Over-lake meteorological observations show large differences for some variables between the 2 yr. Higher air and water temperatures occurred in 1998, particularly in spring and throughout the summer. The warm 1997–98 period resulted in earlier ice breakup compared to a 12-yr record. Large heat gains during the spring in 1998 resulted in higher surface temperatures and lake heat content than in 1999. Although the ice-free periods for both years were longer than the 12-yr mean, there were 27 more ice-free days in 1998 than in 1999. Larger vapor pressure gradients and slightly higher solar radiation input over concurrent periods occurred in 1999; however, the shorter ice-free season in 1999 contributed to lower lake temperatures and heat storage. Rouse et al. (2003) found higher cumulative evaporation in 1998 compared to 1999 related to the extended ice-free period.

Low-level fog has been observed over Great Slave Lake during spring mooring surveys along the cross-lake transect (B. Moore 2002, personal communication). Although there were no specific measurements of over-lake fog by the Coast Guard, fog appears to be a common occurrence in the period after ice melt. The intensive investigation of Lake Ontario during the International Field Year for the Great Lakes (Aubert and Richards 1981) demonstrated that the presence of over-lake fog can be a significant factor that can influence the accuracy of modeling of the lake heat flux, especially in spring (e.g. Schertzer 1997; Schertzer and Croley 1999). Future research is required to assess the effect

of over-lake fog in modeling of lakewide heat fluxes at this time of year on Great Slave Lake.

The observational program in this study supported development and verification of algorithms for remote sensing of temperature (Bussi eres and Schertzer 2003) and net surface solar radiation from AVHRR (Leighton and Feng 2000).

The heat content analysis relied on detailed temperature data from a cross-lake transect and the bathymetry developed for this investigation. There are several factors that could affect the accuracy of the computed heat storage. For example, Fig. 6 showed that surface temperatures at the shallow nearshore site HR are as much as 3°C higher than that midlake during the spring shortly after ice breakup. Further, the lack of flow and temperature data from the Salve River precluded estimates of contributions from this source to lake heating. Considering that the measurement array consists largely of midlake stations, our heat content may contain an underestimate in early spring and an overestimate in the fall because nearshore areas cool faster than those midlake. We note that the same procedures were followed for both 1998 and 1999, which allows an interannual comparison. Other investigations of heat storage in large deep lakes (e.g., Rawson 1950; Schertzer et al. 1987, etc.) have been largely limited to use of ship surveillance data, which are collected at a grid of stations during surveys lasting 1 week and only up to 8–10 times during the ice-free season. With respect to the ship survey scheme over a grid of stations, many years of data are required to derive a mean heat content curve, particularly during the ice-free season (Boyce et al. 1977). The procedure adopted in this paper has the advantage of providing very detailed in situ temperatures with depth from which to approximate a daily heat content and to represent thermal dynamical responses over an annual cycle. Future research is required to assess the effect of unaccounted heat sources on the annual heat content.

We computed a higher heat content in 1998 compared to 1999. The maximum in 1998 occurred nearly 20 days before 1999, due to earlier ice melt. Although the spring heat gain was larger in 1999, compared to that estimated for 1998, the summer heat gain was significantly larger in 1998. Because 1998 was influenced by a record ENSO contributing to higher over-lake air temperatures and a longer ice-free season than previous years, and had air temperature and wind speeds higher than Yellowknife climatic normals, the conditions in 1998 may be considered anomalous. We note that lake heat contents computed in only 2 yr, 1998 and 1999, may not be fully representative of most years. A longer time series is required to analyze the interannual variability for this northern lake. However, this investigation has shown the high sensitivity of the lake to small changes in meteorological conditions and timing of ice breakup and freezeup.

Good correspondence between the bulk heat ex-

change in this paper and the computed heat flux (Rouse et al. 2003) gives confidence in the magnitude and seasonal variability in the surface heat flux and methodology for heat content approximation adopted for this lake. Spatial variability in meteorological components such as over-lake air temperatures, vapor pressures, and wind speed were noted, especially in the early spring. Future research is required to assess the cross-lake variability in the computed heat flux by incorporating the meteorological buoy data, leading to a lakewide flux computation for comparison with the bulk heat exchange. Computation of the lakewide heat flux and variability is important to the development of atmosphere–lake coupled models.

Rawson (1950) cited a number of limitations to his investigation of Great Slave Lake. For example, a limited number of depth soundings allowed only a general description of the lake bathymetry for application to thermal problems. Measurements were constrained to the ice-free period due to use of ship surveys, and this precluded derivation of an annual temperature cycle. Temperature observations were conducted at ~30 main lake stations at approximately weekly intervals, necessitating use of mean values to estimate heat content. Over-lake in situ observations of meteorology and temperature were not conducted and precluded examination of detailed dynamics of the thermal responses to surface forcing at timescales common with current instrumentation. Our investigation during the CAGES period has extended the initial investigation of Rawson (1950) through developing the first computer-compatible 2 km × 2 km bathymetry for this lake, and from detailed description of cross-lake meteorological, radiation, and physical limnological variability. For the first time it details lake temperature and heat content responses over an annual cycle, and indicates the surprising sensitivity of a large northern lake to external larger-scale influences, such as the intense El Ni o, which extended from 1997 to mid-1998.

*Acknowledgments.* Financial support for this research has been received from the Global Energy and Water Cycle Experiment (GEWEX), and from the Aquatic Ecosystem Impacts Research Branch of the National Water Research Institute (NWRI). Additional support has been received by coauthors on various aspects of the investigation. The Research Support Branch (RSB) of NWRI, Engineering Services prepared the instrumentation and preprocessing of data. Deployment, refurbishing, and retrieval of the moorings were conducted by the Technical Operations Services of RSB, NWRI. Special thanks to Barry Moore, Bob Rowsell, and Irwin Smith of NWRI for Technical and Engineering support. Logistical support was provided by the Great Slave Lake branch of the Canadian Coast Guard (Hay River). Thanks to Ron McLaren (MSC, Pacific and Yukon Region) who kindly gave permission for placement of a relative humidity sensor on the OD buoy

and provided access to data. John Gyakum (McGill University), Paul Hamblin, Jim Bull, and Ram Yerubandi of NWRI, and Claire Oswald and Devon Worth (McMaster University) provided useful comments on aspects of the paper.

## REFERENCES

- Aubert, E. J., and T. L. Richards, 1981: *IFYGL—The International Field Year for the Great Lakes*. NOAA Great Lakes Environmental Research Laboratory, 410 pp.
- AXYS, 1996: Meteorological and oceanographic measurements from Canadian weather buoys. AXYS Environmental Consulting Final Rep. SP-070, 72 pp.
- Blanken, P. D., and Coauthors, 2000: Eddy covariance measurements of evaporation from Great Slave Lake, Northwest Territories, Canada. *Water Resour. Res.*, **36**, 1069–1078.
- , —, and W. M. Schertzer, 2003: Enhancement of evaporation from a large northern lake by the entrainment of warm, dry air. *J. Hydrometeorol.*, **4**, 680–693.
- Boyce, F. M., W. J. Moody, and B. L. Killins, 1977: Heat content of Lake Ontario and estimates of average surface heat fluxes during IFYGL. Inland Waters Directorate Tech. Rep. 101, 120 pp.
- , M. A. Donelan, P. F. Hamblin, C. R. Murthy, and T. J. Simons, 1989: Thermal structure and circulation in the Great Lakes. *Atmos.–Ocean*, **27**, 607–642.
- Bussières, N., 2001: The use of thermal AVHRR information in MAGS. *Proc. Fifth Int. Study Conf. on GEWEX in Asia and GAME*, Vol. 2, Nagoya, Japan, GAME International Science Panel, GAME Publication 31(2), 356–360.
- , and W. M. Schertzer, 2003: The evolution of AVHRR-derived water temperatures over lakes in the Mackenzie Basin and hydrometeorological applications. *J. Hydrometeorol.*, **4**, 660–672.
- Derecki, J. A., 1975: Evaporation from Lake Erie. NOAA Tech. Rep. ERL 342-GLERL 3, 84 pp.
- Leighton, H., and J. Feng, 2000: Solar radiation budgets for MAGS. *Proc. GAME-MAGS Int. Workshop*, Nagoya, Japan, Institute for Hydrospheric–Atmospheric Science, Nagoya University, Research Rep. 7, 31–34.
- Oke, T., 1987: *Boundary Layer Climates*. 2d ed. Routledge, 435 pp.
- Pinsak, A. P., and G. K. Rodgers, 1981: Energy balance. *IFYGL—The International Field Year for the Great Lakes*, E. J. Aubert and T. L. Richard, Eds., NOAA Great Lakes Environmental Research Laboratory, 169–197.
- Pruppacher, H. R., and J. D. Klett, 1980: *Microphysics of Clouds and Precipitation*. D. Reidel, 714 pp.
- Rawson, D. S., 1950: The physical limnology of Great Slave Lake. *J. Fish. Res. Board Can.*, **8**, 3–66.
- Rouse, W. R., P. D. Blanken, W. M. Schertzer, and C. Spence, 2000a: The role of lakes in the surface climates of cold regions. *Proc. GAME-MAGS Int. Workshop*, Nagoya, Japan, Institute for Hydrospheric–Atmospheric Science, Nagoya University, Research Rep. 7, 77–80.
- , —, A. K. Eaton, R. M. Petrone, W. M. Schertzer, and C. Spence, 2000b: Energy and water balance of high latitude surfaces. *Proc. Sixth MAGS Workshop for the Mackenzie GEWEX Study (MAGS)*, Saskatoon, SK, Canada, NSERC, AES, Environment Canada, and NWRI, 81–98.
- , and Coauthors, 2002: Energy and water cycles in a high latitude, north-flowing river system: Summary of results from the Mackenzie GEWEX study—Phase I. *Bull. Amer. Meteor. Soc.*, **84**, 73–87.
- , C. M. Oswald, J. Binyamin, P. D. Blanken, W. M. Schertzer, and C. Spence, 2003: Interannual and seasonal variability of the surface energy balance and temperature of central Great Slave Lake. *J. Hydrometeorol.*, **4**, 720–730.
- Schertzer, W. M., 1997: Freshwater lakes. *The Surface Climates of Canada*, W. G. Bailey, T. E. Oke, and W. R. Rouse, Eds., McGill-Queens University Press, 124–148.
- , 2000: Digital bathymetry of Great Slave Lake. NWRI Contribution No. 00-257, 66 pp.
- , and T. E. Croley II, 1999: Climate and lake responses. *Potential Climate Change Effects on Great Lakes Hydrodynamics and Water Quality*, D. C. L. Lam and W. M. Schertzer, Eds., American Society of Civil Engineers Press, 1–74.
- , J. H. Saylor, F. M. Boyce, D. G. Robertson, and F. Rosa, 1987: Seasonal thermal cycle of Lake Erie. *J. Great Lakes Res.*, **13**, 468–486.
- , W. R. Rouse, and P. D. Blanken, 2000a: Cross-lake variation of physical limnological and climatological processes of Great Slave Lake. *Phys. Geogr.*, **21**, 385–406.
- , —, and —, 2000b: Modelling of large lakes in cold regions. *Proc. GAME-MAGS Int. Workshop*, Nagoya, Japan, Institute for Hydrospheric–Atmospheric Science, Nagoya University, Research Rep. 7, 126–129.
- Stewart, R. E., and Coauthors, 1998: The Mackenzie GEWEX Study: The water and energy cycles of a major North American river system. *Bull. Amer. Meteor. Soc.*, **79**, 2665–2683.
- U.S. Army Corps of Engineers, 1984: Shore Protection Manual. Vol. 1. 4th ed. U.S. Army Corps of Engineers, Coastal Engineering Research, 608 pp.
- van der Leeden, F., F. L. Troise, and D. K. Todd, 1990: *The Water Encyclopedia*. Lewis, Inc., 880 pp.
- Walker, A. E., and M. R. Davey, 1993: Observation of Great Slave Lake ice freeze-up and break-up processes using passive microwave satellite data. *Proc. 16th Symp. on Remote Sensing*, Sherbrooke, QC, Canada, L'AQT/CRSS, 233–238.
- , A. Silis, J. Metcalf, M. Davey, R. Brown, and B. Goodison, 1999: Snow cover and lake ice determination in the MAGS region using passive microwave satellite and conventional data. *Proc. Fourth Scientific Workshop for the Mackenzie GEWEX Study (MAGS)*, Montreal, QC, Canada, NSERC and AES, Environment Canada, 89–91.

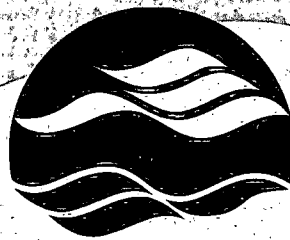
Environment Canada Library, Burlington



3 9055 1018 1958 8



**National Water Research Institute**  
**Environment Canada**  
**Canada Centre for Inland Waters**  
P.O. Box 5050  
867 Lakeshore Road  
Burlington, Ontario  
L7R 4A6 Canada



**NATIONAL WATER  
RESEARCH INSTITUTE**  
**INSTITUT NATIONAL DE  
RECHERCHE SUR LES EAUX**

**Institut national de recherche sur les eaux**  
**Environnement Canada**  
**Centre canadien des eaux intérieures**  
Case postale 5050  
867, chemin Lakeshore  
Burlington, Ontario  
L7R 4A6 Canada

**National Hydrology Research Centre**  
11 Innovation Boulevard  
Saskatoon, Saskatchewan  
S7N 3H5 Canada

**Centre national de recherche en hydrologie**  
11, boul. Innovation  
Saskatoon, Saskatchewan  
S7N 3H5 Canada